Poisson ratio in composites of auxetics

Gaoyuan Wei[1,2,*] and S. F. Edwards[1]
[1]*Polymers and Colloids Group, Cavendish Laboratory, University of Cambridge, Madingley Road, Cambridge CB3 0HE, United Kingdom*
[2]*Department of Polymer Science and Engineering and Institute of Polymer Science, College of Chemistry and Molecular Engineering, Peking University, Beijing 100871, People's Republic of China*
(Received 1 June 1998)

Mean-field theory of elastic moduli of a two-phase disordered composite with ellipsoidal inclusions is reviewed together with an indication as to how interactions among inclusions may be taken into account. In the mean-field approximation, the effective Poisson ratio σ_e in composites with auxetic inclusions of various shapes such as discs, spheres, blades, needles, and disks is studied analytically and numerically. It is shown that phase properties such as inclusion volume or area fraction ϕ and matrix and inclusion Poisson ratios (σ_m and σ) and Young's moduli (E_m and E) have a marked effect on σ_e. The earlier theoretical findings of the existence of auxeticity windows and the widening effect of inclusion-inclusion interactions on the window for $\delta=E/E_m$ are reconfirmed for composites of auxetic spheres in both two and three dimensions, with new auxeticity windows discovered for the other inclusion shapes. For a composite with $\sigma=-0.8$, $\sigma_m=0.25$, and $\phi=0.4$, it is found that the sphere is the most σ_e-lowering or negative-σ_e-producing inclusion shape for δ around 1/2, while disklike inclusions yield a most negative σ_e for δ greater than 1. [S1063-651X(98)03911-7]

PACS number(s): 61.41.+e, 62.20.Dc, 62.90.+k, 89.90.+n

I. INTRODUCTION

The appearance of man-made auxetics [1,2], i.e., materials with negative Poisson ratios, has led to the study of auxetic composites [3]. In this paper we study the Poisson ratio of a special class of composites with auxetic inclusions, which are believed to be of potential technological significance.

The paper is organized as follows. The general mean-field theory of effective elastic moduli of a two-phase disordered composite is first reviewed along with corrections to the mean-field results that take into account two- and three-body interactions among the inclusions. Analytic and numerical results are then presented for auxetic inclusions having spherical, needlelike, and disklike shapes. Finally, a discussion of the results obtained and some conclusions are given.

II. MEAN-FIELD THEORY

In calculating effective elastic moduli of a solid suspension of spheres with a spherically symmetric elastic profile, a mean-field approximation that corresponds to the Lorentz local field in the theory of dielectrics was presented in 1992 by Felderhof and Iske [4]. The resulting expressions for the effective bulk modulus κ_e and shear modulus μ_e in the case of uniform spheres reduce to those of Weng [5] and Markov [6] by use of the Mori-Tanaka mean-field theory [7–9] and Eshelby's theoretical conclusion [10] that there exists a uniform strain field inside an ellipsoidal inclusion that is algebraically related to the matrix or host strain. In this section we review the general mean-field theory of effective elastic properties for ellipsoidal inclusions along the lines followed by Reynolds and Hough [11] in the case of dielectrics and later by Berryman and Berge [9] for elastic composites and indicate how corrections to the mean-field results may be added.

Let us begin with a derivation of effective dielectric constant ε_e of an isotropic N-phase composite. The assumption of macroscopic homogeneity of the composite medium and perfect bonding between phases leads to the following rules of mixture for average electric displacement $\mathbf{D}$ and field $\mathbf{E}$ of the composite:

$$\mathbf{D}=\sum_{i=1}^{N}\phi_i\mathbf{D}_i \tag{1}$$

and

$$\mathbf{E}=\sum_{i=1}^{N}\phi_i\mathbf{E}_i, \tag{2}$$

where ϕ_i, $\mathbf{D}_i$, and $\mathbf{E}_i$ are the volume fraction, electric displacement, and field of the ith phase with $\mathbf{D}_i=\varepsilon_i\mathbf{E}_i$ and $\mathbf{D}=\varepsilon_e\mathbf{E}$, which further yield

$$\sum_{i=1}^{N}\phi_i(\varepsilon_i-\varepsilon_e)\mathbf{E}_i=\mathbf{0}. \tag{3}$$

The mean-field approximation requires that the homogeneous electric field $\mathbf{E}_i$ $(i=1,2,\ldots,N-1)$ inside the ith isotropic ellipsoidal inclusions [12] be algebraically related to the external field $\mathbf{E}_N$ of the isotropic matrix as

$$\mathbf{E}_i=R_{iN}\mathbf{E}_N, \tag{4}$$

where R_{iN} is given by

$$R_{iN}=(1/d)\sum_{j=1}^{d}[1+L_j(\varepsilon_i/\varepsilon_N-1)]^{-1}, \tag{5}$$

*Author to whom correspondence should be addressed.
FAX: 86-10-62751708.
Electronic address: gywei@chemms.chem.pku.edu.cn

with L_j denoting the jth depolarizing factor of the ellipsoid [12–17] and d the dimensionality of space in which the composite resides. Substitution of Eq. (4) in Eq. (3) then gives

$$\sum_{i=1}^{N-1} \phi_i(\varepsilon_i-\varepsilon_e)R_{iN}=0, \tag{6}$$

which, for a two-phase composite [11,17], reduces to

$$\varepsilon_e=(\phi_m\varepsilon_m+\phi\varepsilon R)/(\phi_m+\phi R), \tag{7}$$

where the subscript m denotes a matrix with $\phi=1-\phi_m$ and R is the same as R_{iN} but with $\varepsilon_i/\varepsilon_N$ replaced by $\varepsilon/\varepsilon_m$ in Eq. (5). We notice that ε_e as given by Eq. (7) obeys a generalized rule of mixture [3], i.e., Eq. (7) can be rewritten as $\varepsilon_e=r_m\varepsilon_m+(1-r_m)\varepsilon$, with $r_m=\phi_m/(\phi_m+\phi R)\in[0,1]$, and it reduces to the well-known Clausius-Mossotti formula [4] for spherical inclusions. We further note that when N is replaced by e in Eq. (4), one gets a governing equation for ε_e that is recognized as the effective medium approximation [16,18] or the self-consistent scheme [9].

For an analogous derivation of effective elastic moduli, the average field variables that obey the rules of mixture are the stress and strain fields denoted by $\boldsymbol{\sigma}$ and $\boldsymbol{\varepsilon}$, respectively, with $\boldsymbol{\sigma}=\mathbf{L}_e\boldsymbol{\varepsilon}$, $\boldsymbol{\varepsilon}=\mathbf{M}_e\boldsymbol{\sigma}$, and $\mathbf{M}_e\mathbf{L}_e=\mathbf{I}=\mathbf{L}_e\mathbf{M}_e$, where $\mathbf{L}_e$ and $\mathbf{M}_e$ are the effective stiffness and compliance tensors, respectively, and $\mathbf{I}$ is the identity tensor or [19] a 6×6 unit matrix. Use of these relations and similar ones between $\boldsymbol{\sigma}_i$ and $\boldsymbol{\varepsilon}_i$ for the ith phase yields

$$\sum_{i=1}^{N} \phi_i(\mathbf{L}_i-\mathbf{L}_e)\boldsymbol{\varepsilon}_i=\mathbf{0} \tag{8}$$

and

$$\sum_{i=1}^{N} \phi_i(\mathbf{M}_i-\mathbf{M}_e)\boldsymbol{\sigma}_i=\mathbf{0}. \tag{9}$$

The mean-field approximation in this case is tantamount to assuming that

$$\boldsymbol{\varepsilon}_i=\mathbf{A}_{iN}\boldsymbol{\varepsilon}_N \tag{10}$$

and

$$\boldsymbol{\sigma}_i=\mathbf{B}_{iN}\boldsymbol{\sigma}_N, \tag{11}$$

where $\mathbf{B}_{iN}=\mathbf{L}_N\mathbf{A}_{iN}\mathbf{M}_i$ and $\mathbf{A}_{iN}$ is the Wu tensor $\mathbf{T}_{iN}$ [9,20], which is related to the Eshelby tensor $\mathbf{S}$ [10] by [8]

$$\mathbf{T}_{iN}=[\mathbf{I}+\mathbf{S}\mathbf{L}_i^{-1}(\mathbf{L}_N-\mathbf{L}_i)]^{-1}, \tag{12}$$

whose isotropic average is [9,20]

$$T_{ijkl}=(1/d)(P-Q)\delta_{ij}\delta_{kl}+(Q/2)(\delta_{ik}\delta_{jl}+\delta_{il}\delta_{jk}), \tag{13}$$

where scalars P and Q may be analytically expressed in the case of spheroidal inclusions [8,9,20,21] and are generally dependent on depolarizing or demagnetizing factors of the ellipsoid. Substitution of Eq. (10) in Eq. (8) then gives [6,8,9]

$$\sum_{i=1}^{N-1} \phi_i(\mathbf{L}_i-\mathbf{L}_e)\mathbf{T}_{iN}=\mathbf{0}, \tag{14}$$

which, for an isotropic composite made of isotropic ellipsoidal inclusions embedded in an isotropic matrix, reduces to [3]

$$\kappa_e=(\phi_m\kappa_m+\phi\kappa P)/(\phi_m+\phi P) \tag{15}$$

and

$$\mu_e=(\phi_m\mu_m+\phi\mu Q)/(\phi_m+\phi Q), \tag{16}$$

where the expression of $\mathbf{L}$ for isotropic materials, i.e., $L_{ijkl}=(\kappa-d/2)\delta_{ij}\delta_{kl}+\mu(\delta_{ik}\delta_{jl}+\delta_{il}\delta_{jk})$, has been used. Equations (15) and (16), when explicit expressions of P and Q for spherical inclusions are used, yield the mean-field results of Markov [6], Weng [5], Felderhof and Iske [4], and Torquato [22]. Furthermore, κ_e and μ_e as calculated from the above equations are known to fall within or coincide with the Hashin-Shtrikman-Walpole bounds [4,23]. We note that as in the case of dielectrics, the replacement of N by e in Eqs. (10) and (11) results in the analogous effective medium or coherent potential approximation to κ_e and μ_e [9].

A correction to the mean-field approximation to ε_e was carried out by Kirkwood [24] and later by Brown [25], Felderhof *et al.* [4,26], and Sen and Torquato [27], among others. An analogous result for κ_e and μ_e has recently been presented by Torquato [22] for any arrangement of spherical inclusions within a matrix and for any d. For isotropic ellipsoidal inclusions in an isotropic matrix, we find that the expansion parameters in the Kirkwood-Brown-Torquato expansion of some chosen function of one of effective properties are changed to $1-R$ in the dielectric case and $1-P$ and $1-Q$ in the elastic case, i.e.,

$$\phi^2[\varepsilon-\varepsilon_m+(1-R)(\varepsilon_e-\varepsilon)]/(\varepsilon_e-\varepsilon_m) = \phi-\sum_{n=3}^{\infty} C_n(1-R)^{n-1}, \tag{17}$$

$$\phi^2[\kappa-\kappa_m+(1-P)(\kappa_e-\kappa)]/(\kappa_e-\kappa_m) = \phi-\sum_{n=3}^{\infty}\sum_{m=0}^{n-1} A_{nm}R_{nm}, \tag{18}$$

and

$$\phi^2[\mu-\mu_m+(1-Q)(\mu_e-\mu)]/(\mu_e-\mu_m) = \phi-\sum_{n=3}^{\infty}\sum_{m=0}^{n-1} B_{nm}R_{nm}, \tag{19}$$

where $R_{nm}=(1-P)^m(1-Q)^{n-m-1}$ and A_{nm}, B_{nm}, and C_n are coefficients yet to be determined (see Refs. [22,27] for explicit expressions of these coefficients in the case of spheres) and are all zero in the mean-field approximation. We note that the truncation of the above series at $n=3$ yields corrections to the mean-field results that take into account two- and three-body interactions among inclusions and have been used by Wei and Edwards [3] in a study of composites of auxetic spheres.

With κ_e and μ_e known, the effective Young modulus E_e and Poisson ratio σ_e may be calculated by use of

$$\sigma_e=(d\kappa_e-2\mu_e)/[d(d-1)+2\mu_e] \tag{20}$$

and

$$E_e=2\mu_e(1+\sigma_e)=d\kappa_e[1+(1-d)\sigma_e] \tag{21}$$

for any $d\geqslant 2$, which may be readily proved in the framework of classical elasticity theory. We note that in general one has $-1\leqslant\sigma_e\leqslant 1/(d-1)$ and $0\leqslant E_e\leqslant\infty$ or [9,28]

$$\sigma_e(\kappa_{e,L},\mu_{e,U})\leqslant\sigma_e(\kappa_e,\mu_e)\leqslant\sigma_e(\kappa_{e,U},\mu_{e,L}) \tag{22}$$

and

$$E_e(\kappa_{e,L},\mu_{e,L})\leqslant E_e(\kappa_e,\mu_e)\leqslant E_e(\kappa_{e,U},\mu_{e,U}), \tag{23}$$

where $\kappa_{e,L}$ and $\kappa_{e,U}$ are lower and upper bounds of κ_e, respectively. We further note that in the mean-field approximation E_e and σ_e obey generalized rules of mixture only when $\kappa=\kappa_m$ or $\mu=\mu_m$, with $\sigma_e=\phi_m\sigma_m+(1-\phi_m)\sigma\equiv\langle\sigma\rangle$ and $E_e=\langle E\rangle$ for $\mu=\mu_m$ and $d=2$. For κ_e and μ_e given by Eqs. (15) and (16), in particular, we have from Eq. (20)

$$\sigma_e=(\sigma_m s_m\phi_m^2+\sigma s\phi^2PQ-\beta_1\phi\phi_m)/(s_m\phi_m^2+s\phi^2PQ+\beta_2\phi\phi_m), \tag{24}$$

where $s_m\equiv s(\sigma_m)$, $s\equiv s(\sigma)$, and $s(\sigma)$ and β_n are given by

$$s(\sigma)=d(1+\sigma)^{-1}[1+\sigma(1-d)]^{-1} \tag{25}$$

and

$$\beta_n=Qs_n(\sigma_m,\sigma,\delta)+\delta Ps_n(\sigma,\sigma_m,\delta^{-1}), \tag{26}$$

with $\delta=E/E_m$ and $s_n(\sigma_m,\sigma,\delta)$ defined as

$$s_n(\sigma_m,\sigma,\delta)=\delta/(1+\sigma)+[d(n-1)-1]/[1+\sigma_m(1-d)]. \tag{27}$$

We note that the denominator in Eq. (24) is positive as both P and Q are non-negative and the numerator is quadratic in ϕ, which yields one meaningful root of σ_e as

$$\phi_c=[\rho_m+\beta_1/2-(\beta_1^2/4-\rho\rho_m\delta PQ)^{1/2}]/(\rho_m+\beta_1+\rho\delta PQ) \tag{28}$$

where $\rho=\sigma s$ and $\rho_m=\sigma_m s_m$. In particular, for $\sigma\sigma_m\leqslant 0$, e.g., $\sigma_m\geqslant 0$ and $\sigma\leqslant 0$, we have $-1\leqslant\sigma_e\leqslant 0$ if $\phi_c\leqslant\phi\leqslant 1$. In other words, an auxetic composite results when ϕ exceeds a critical value as revealed in a study of auxetic composites [3].

III. SHAPE EFFECT

The effect of the inclusion shape on effective elastic moduli of a composite material has been investigated extensively in the past [8,10,17,20,21,29–36]. In this section we study this shape effect on the effective Poisson ratio by concentrating our attention on three distinctive types of inclusion shapes, spheres, needles, and disks, for which the depolarizing factors are very simple [9,13], i.e., (1/3,1/3,1/3), (0,1/2,1/2), and (0,0,1), respectively, while those of the two-dimensional analogs, i.e., discs and blades, are (1/2,1/2) and (0,1). From these factors the Eshelby tensor and hence the Wu tensor can be easily written down, which then yields analytic expressions for R, P, and Q appearing in the mean-field equations for ε_e, κ_e, and μ_e. For d-dimensional spheres, it is shown by Torquato [22,27] that $R=1/F(d,\varepsilon/\varepsilon_m)$, $P=1/F(d,\kappa/\kappa_m)$, and $Q=1/F(d,\mu/\mu_m)$, with $F(d,x)$ defined as

$$F(d,x)=1+(x-1)/G(x,\gamma_m), \tag{29}$$

where $G(x,\gamma_m)=d,\ 1+2(1-1/d)\gamma_m$, and $(1+d/2)[1-(2/d)/(2+1/\gamma_m)]$ for $x=\varepsilon/\varepsilon_m$, κ/κ_m, and $\mu/\mu_m\equiv\gamma$, respectively, with $\gamma_m=\mu_m/\kappa_m$. For $d=2$ and 3 in particular we have

$$P^{-1}=\begin{cases}(1-\sigma_m)[1+\delta(1+\sigma_m)/(1-\sigma)]/2 & (d=2)\\ (1-2\sigma_m)[2+\delta(1+\sigma_m)/(1-2\sigma)]/3(1-\sigma_m) & (d=3)\end{cases} \tag{30}$$

and

$$Q^{-1}=\begin{cases}(1+\sigma_m)[1+\delta(3-\sigma_m)/(1+\sigma)]/4 & (d=2)\\ [7-5\sigma_m+2\gamma(4-5\sigma_m)]/15(1-\sigma_m) & (d=3).\end{cases} \tag{31}$$

In the calculation of the corrections to the mean-field results such as those carried out by Torquato [22] and Wei and Edwards [3], analytic expressions for the coefficients A_{3m} and B_{3m} that depend also on ϕ and the geometric arrangements of spheres may be found in Refs. [37–39]. For d-dimensional needles, we find [9,20,34]

$$P=\begin{cases}(1-\sigma)[1+\delta^{-1}(1+\sigma)/(1-\sigma_m)]/2 & (d=2)\\ (1/3)[1+\gamma/(1-2\sigma)]^{-1}[\gamma+(5-4\sigma_m)/(1-2\sigma_m)] & (d=3)\end{cases} \tag{32}$$

and

$$Q=\begin{cases}(1+\sigma)[1+\delta^{-1}(3-\sigma)/(1+\sigma_m)]/4 & (d=2)\\ (8/5)(1-\sigma_m)/[1+\gamma(3-4\sigma_m)]+(2/15)(1+\gamma)^{-1}(1+\gamma-2\sigma)^{-1}\{8(1-2\sigma)+\gamma[3(3-\sigma)+\delta(1+\sigma_m)]\} & (d=3),\end{cases} \tag{33}$$

TABLE I. Critical volume fraction at $\delta=4/5$ and critical Young modulus ratios at $\phi=0.45$ for the onset of auxeticity in composites of auxetic ($\sigma=-0.9$) inclusions of various shapes. Cases 1, 2 and 3 correspond to $\sigma_m=0.45$, 0.30, and 0.15, respectively. For case 2 there is an additional auxeticity window for disks, i.e., $0<\delta<0.0231$.

	ϕ_c			δ_{c1},δ_{c2}		
Shape	Case 1	Case 2	Case 3	Case 1	Case 2	Case 3
Disc	0.3173	0.2366	0.1342	0.0309,2.301	0.0230,3.794	0.0171, 6.834
Sphere	0.4647	0.3258	0.1731		0.0905,4.323	0.0342,11.18
Blade	0.4065	0.2933	0.1617	0,5.410	0,17.46	0,28.21
Needle	0.5879	0.3679	0.1818		0.0957,12.93	0.0309,31.16
Disk	0.5677	0.2733	0.1171	0.0069,1.845	0.1541,∞	0,∞

while for three-dimensional disks we have [8,9,20,21]

$$P=(1-2\sigma)[2+\delta^{-1}(1+\sigma)/(1-2\sigma_m)]/3(1-\sigma) \tag{34}$$

and

$$Q=[7-5\sigma+2\gamma^{-1}(4-5\sigma)]/15(1-\sigma). \tag{35}$$

We note that the above expressions for P may be reexpressed as a single one as

$$P^{-1}=1+(\kappa/\kappa_m-1)/\{1+2(d-1)\xi^{-1}[1+C(\gamma-1)]\}, \tag{36}$$

where $\xi=d\kappa_m/\mu_m$ and $C=0$, 1/4, and 1 for spheres and discs (spheres for $d=2$), needles, and disks and blades (needles for $d=2$), respectively (see also Ref. [29]). Equation (36) provides a means for determining inclusion shapes by the measuring of effective bulk modulus of a composite with known composition and elastic moduli of the two isotropic phases as in the case of dielectrics [40].

With explicit expressions for P and Q for spheres, needles, and disks now at hand, one may calculate the effective Poisson ratios of composites with both auxetic and conventional inclusions according to Eq. (24). Here we focus on auxetic inclusions with the more general case left for a future work. Before presenting numerical results on σ_e as calculated from Eq. (24), however, several interesting special cases may be treated analytically. The first one is that of

TABLE II. Effective Poisson ratio and Young modulus ratio for composites of auxetic ($\sigma=-0.9$) inclusions of various shapes with $\sigma_m=0.25$ and $\phi=0.45$.

	$\delta=1/10$		$\delta=1$		$\delta=10$	
Shape	σ_e	δ_e	σ_e	δ_e	σ_e	δ_e
Disc	−0.3020	0.6158	−0.2856	1.125	0.1216	1.943
Sphere	−0.0624	0.8291	−0.2081	1.435	0.0650	2.236
Blade	−0.2679	0.6438	−0.2266	1.172	−0.0508	3.220
Needle	−0.0555	0.8350	−0.1714	1.570	−0.0562	2.999
Disk	−0.0385	0.8497	−0.3575	2.108	−0.7387	6.699

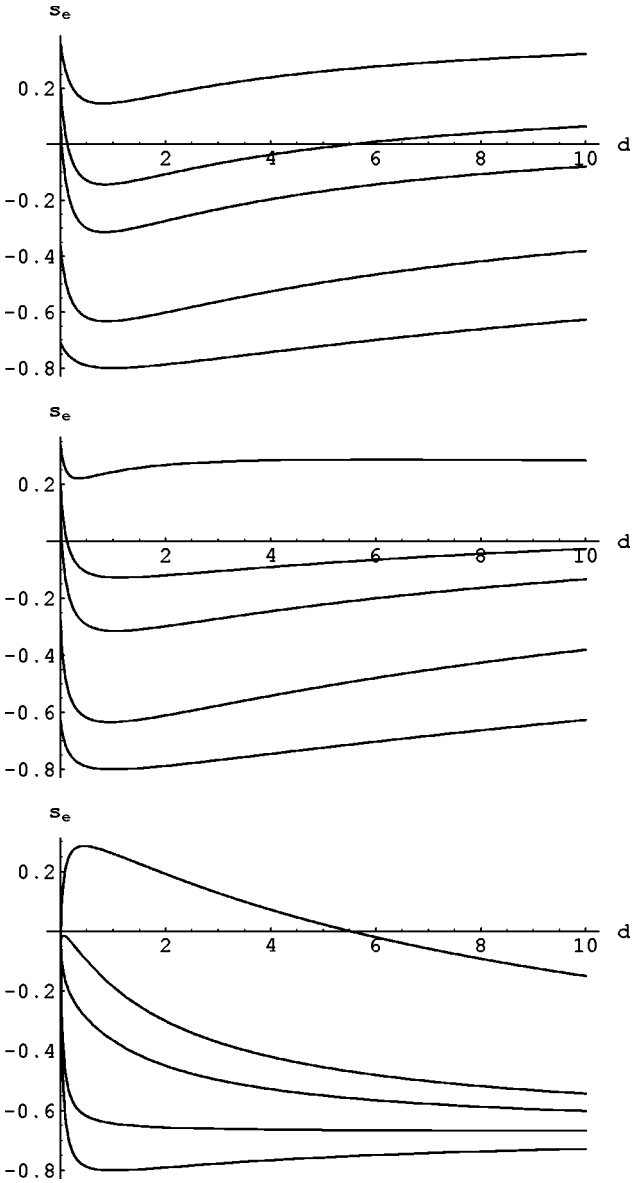

FIG. 1. Plots of the effective Poisson ratio σ_e as a function of the Young modulus ratio δ for three inclusion shapes: a sphere (top), needle (middle), and disk (bottom), with a Poisson ratio σ of -0.8 and a volume fraction ϕ of 0.4. For each of the three cases, the curves from top to bottom correspond to $\sigma_m=0.45,0.2,0$, -0.5, and -0.8, respectively.

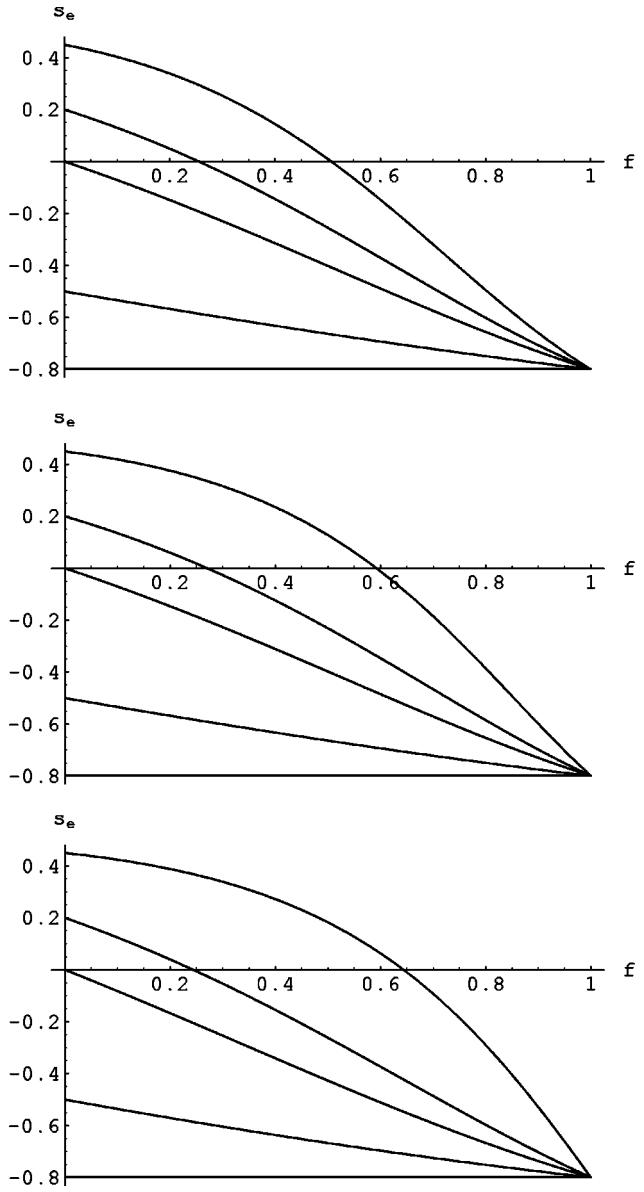

FIG. 2. Plots of σ_e vs ϕ with $\sigma=-0.8$ and $\delta=0.8$, otherwise the same as in Fig. 1.

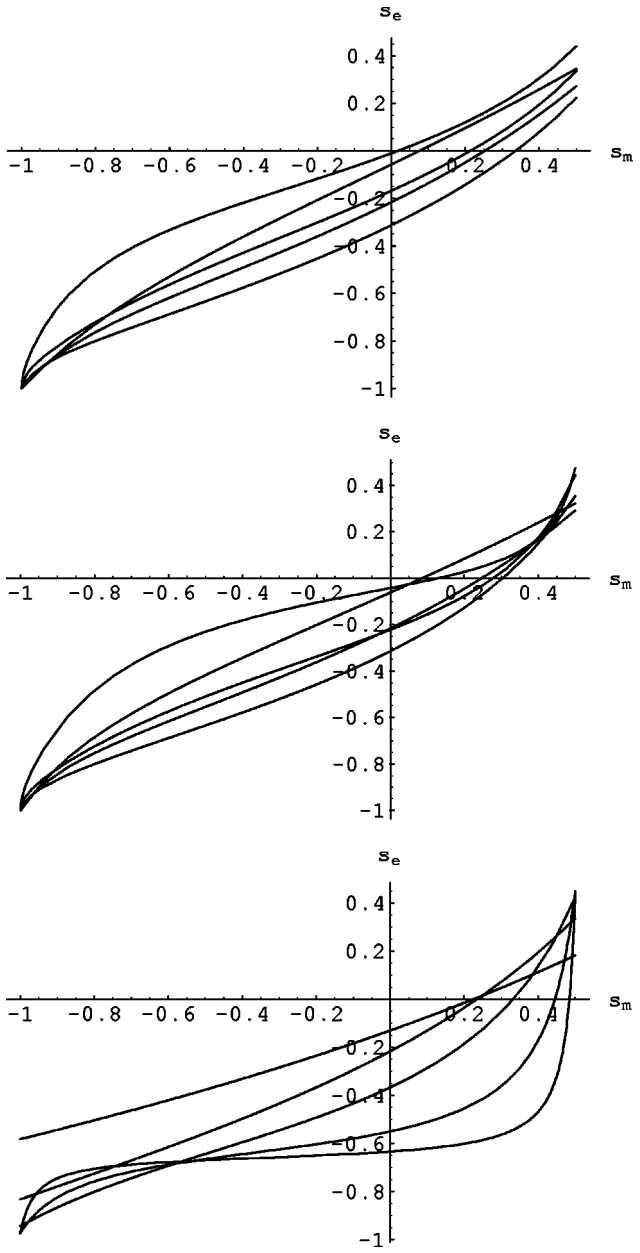

FIG. 3. Plots of σ_e vs σ_m with $\sigma=-0.8$ and $\phi=0.4$, otherwise the same as in Fig. 2, except for the assignments of various values of δ for each curve. Curves from left to right on the $\sigma_e=0$ line correspond to $\delta=20,1/20,5,1/5$, and 1 for spheres, $\delta=1/20,20,1/5,5$, and 1 for needles, and $\delta=1/20,1/5,1,5$, and 20 for disks.

equal shear rigidities of both inclusions and matrix, which was studied by Hill [19], who found that for $d=3$ and arbitrary inclusion shapes,

$$\sigma_e=(\langle\sigma\rangle-\sigma\sigma_m)/(1-\langle\sigma^*\rangle)$$
$$=\langle\sigma\rangle+\phi\phi_m(\sigma-\sigma_m)^2/(1-\langle\sigma^*\rangle), \tag{37}$$

which is greater than or equal to $\langle\sigma\rangle$ as opposed to the equality existing for $d=2$ and may be readily proved with the use of Eqs. (24) and (30)–(35). Here $\langle\sigma^*\rangle\equiv\phi_m\sigma+\phi\sigma_m$. Another shape-independent quantity is the coefficient of $(\delta-1)^2$ in the expansion of σ_e in $\delta-1$ for $\sigma=\sigma_m$, i.e.,

$$\sigma_e=\sigma+\phi\phi_m C_d(\delta-1)^2+O((\delta-1)^3) \tag{38}$$

and

$$C_d=\begin{cases}(1-\sigma^2)(1-3\sigma)/8 & (d=2)\\ (1+\sigma)(1-2\sigma)(1-5\sigma)/15(1-\sigma) & (d=3),\end{cases} \tag{39}$$

which is greater or less than zero according to whether σ is less or greater than $1/(2d-1)$ for any $d\geqslant 2$. We note that $\sigma_e=1/(2d-1)$ if $\sigma=\sigma_m=1/(2d-1)$ for blades, disks, and any d-dimensional spheres while for needles σ_e is in the vicinity of 1/5 when $\sigma=\sigma_m=1/5$. For $\delta=1$, $\sigma=-\sigma_m$ and $\phi=1/2$, we find that σ_e increases monotonically from 0 to a

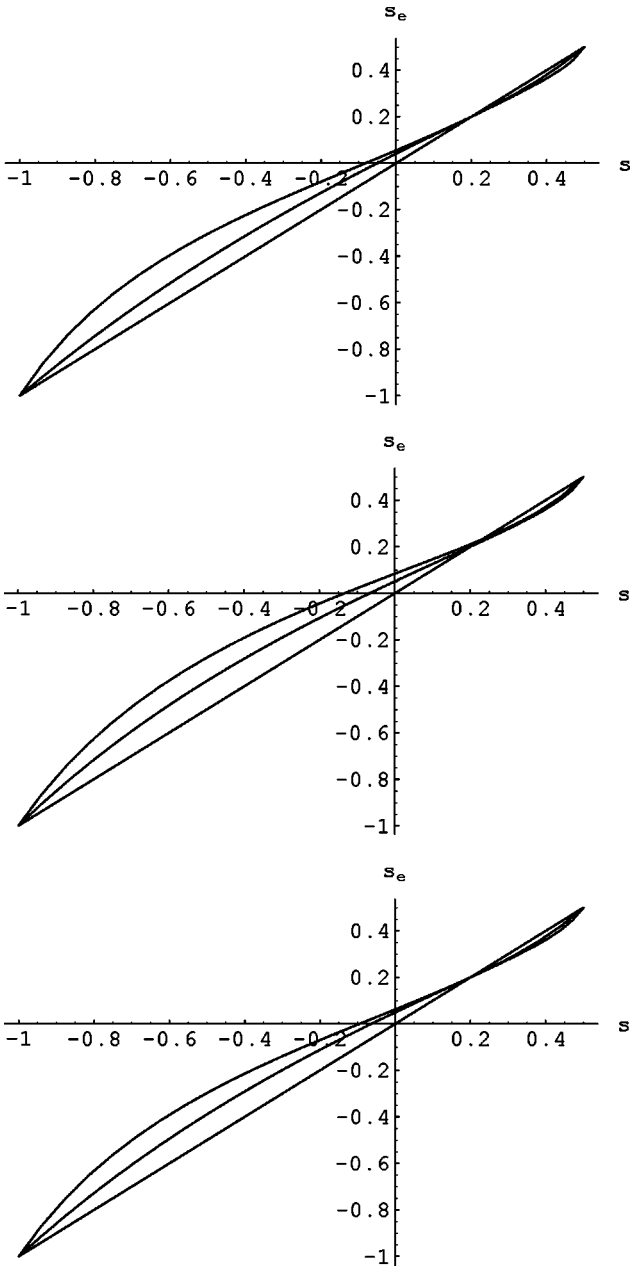

FIG. 4. Plots of σ_e vs $\sigma=\sigma_m$ with $\phi=0.4$, otherwise the same as in Fig. 3, except for the values of δ corresponding to each curve: 10, 1/10, and 1 for spheres and needles and 1/10, 10, and 1 for disks.

certain value less than $1/(d-1)$ as σ_m increases from 0 to $1/(d-1)$ for all the inclusion shapes but disks, for which one has

$$\sigma_e=(\sigma_m^2/2)(1-\sigma_m)/(4+\sigma_m-2\sigma_m^2), \tag{40}$$

which attains a maximum value of 0.019 758 1 at $\sigma_m=0.700\,553$ and a minimum one of 0 at $\sigma_m=0$ and 1. In particular, for spherical inclusions and for $\delta=1$ and $\sigma_m=0$ we have $\sigma_e=\phi\sigma A_d(\sigma,\phi)$ with $A_d(\sigma,\phi)>0$ for $d=2$ and 3 and for $\sigma=-1$ and $\sigma_m=1/(d-1)$,

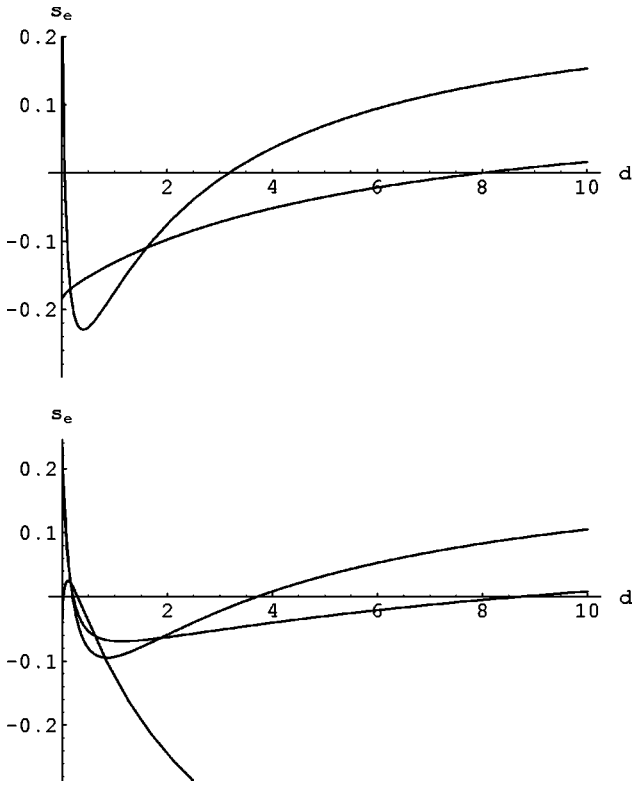

FIG. 5. Comparison of the dependence of σ_e on δ among various inclusion shapes: a disc and blade (top) and a sphere, needle, and disk (bottom), with $\sigma=-0.8$, $\sigma_m=0.25$, and $\phi=0.4$. The curves from top to bottom on the $\delta=6$ line correspond to a disc and blade in the upper figure and a sphere, needle, and disk in the lower, respectively.

$$\sigma_e=\begin{cases}(\delta\phi_m-3\phi+1)/(\delta\phi_m+2\phi^2-\phi+1) & (d=2)\\ (\delta\phi_m+\phi^2-10\phi+4)/(2\delta\phi_m+11\phi^2-14\phi+8) & \\ (d=3), & \end{cases} \tag{41}$$

which may be solved for ϕ_c and δ_c such that when $\phi_c<\phi<1$ and $0<\delta<\delta_c$ one has $\sigma_e<0$, as done by Wei and Edwards [3].

In Table I auxeticity windows, i.e., $(\phi_c,1)$ and $(\delta_{c1},\delta_{c2})$, are displayed for disks and both two- and three-dimensional needles and spheres with $\delta=4/5$ for ϕ_c and $\phi=0.45$ for δ_{c1} and δ_{c2}. Numerical values of σ_e and δ_e for composites of auxetic ($\sigma=-0.9$) inclusions of these five types of shapes with $\sigma_m=0.25$ and $\phi=0.45$ are tabulated in Table II. Figures 1–3 show plots of σ_e as a function of δ, ϕ, and σ_m, respectively, for auxetic ($\sigma=-0.8$) spherical, needlelike, and disklike inclusions when other parameters are fixed, while Fig. 4 plots σ_e vs $\sigma=\sigma_m$ with $\phi=0.4$ for three values of δ: 1/10,1, and 10. In Figs. 5 and 6 the dependence of σ_e on d at $\phi=0.4$ is compared among the five types of inclusion shapes for $\sigma=-0.8$ and $\sigma_m=0.25$, and $\sigma=\sigma_m=-0.5$, respectively. Finally, the effects of weak interactions [3,22] among spherical inclusions on the dependence of σ_e on δ are illustrated in Fig. 7.

IV. DISCUSSION AND CONCLUSION

The existence of auxeticity windows in composites of auxetics was demonstrated by Wei and Edwards [3] for

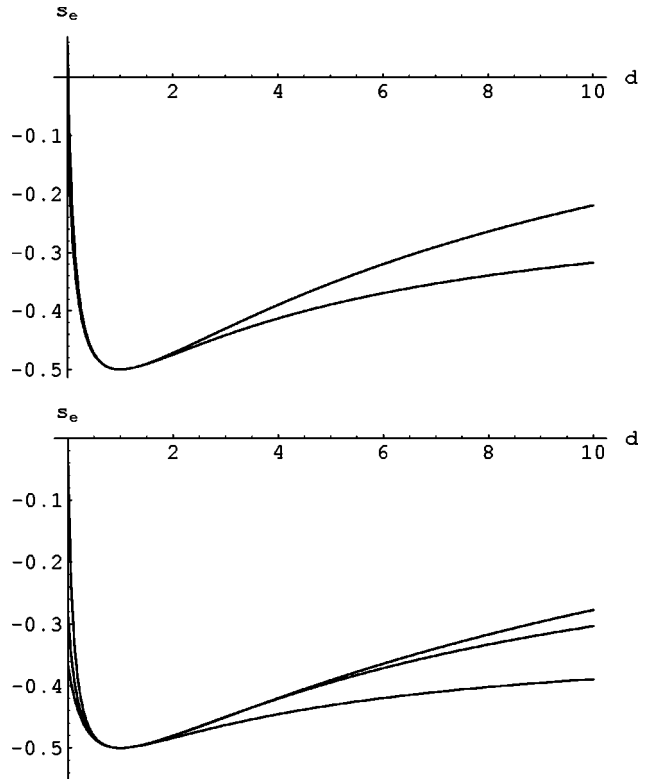

FIG. 6. Plots of σ_e vs δ with $\sigma=\sigma_m=-0.5$ and $\phi=0.4$, otherwise the same as in Fig. 5, except for the assignments of inclusion shapes corresponding to each curve: a blade and disc in the upper figure and a needle, sphere, and disk in the lower, respectively.

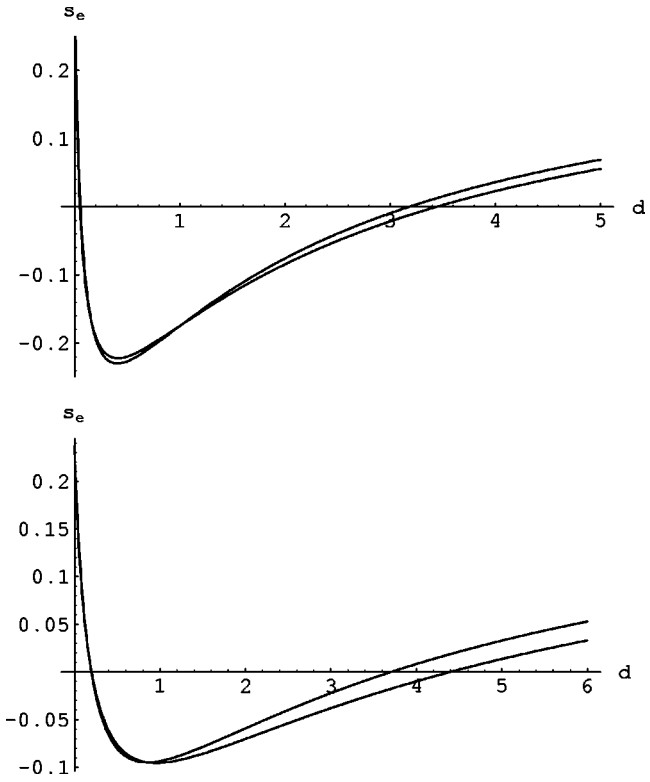

FIG. 7. Illustrations of the effects of weak interactions among spherical inclusions on the dependence of σ_e on δ with $\sigma=-0.8$, $\sigma_m=0.25$, and $\phi=0.4$. The curves from bottom to top on the $\delta=4$ line in both the upper (disc) and lower (sphere) figures correspond to the mean-field result with and without the interaction effects being taken into account, respectively.

spherical inclusions. It is seen from Table I that this is also the case for other inclusion shapes. For $\delta=4/5$, the critical volume fraction ϕ_c above which the composite exhibits auxeticity decreases as σ_m decreases from 0.45 to 0.15 for all the inclusion shapes with $\sigma=-0.9$, but at a given value of σ_m it varies considerably for different inclusion shapes, with ϕ_c for discs being smaller than that for blades in all three cases considered and the smallest ϕ_c being produced by spheres at $\sigma_m=0.45$ and disks at $\sigma_m=0.30$ and 0.15. We notice that ϕ_c for needles are the largest in both two and three dimensions. For $\phi=0.45$, there exists at least one auxeticity window for δ in all the three cases and for all the inclusion shapes except for spheres and needles in case 1 for which no such window is found. It is also seen that δ_{c1} is either zero or close to zero in all the cases and that disklike inclusions gives the largest auxeticity window at $\sigma_m=0.30$ and 0.15. The magnitude of the effective Poisson ratio σ_e and Young modulus ratio δ_e for $\sigma=-0.9$, $\sigma_m=0.25$, and $\phi=0.45$ vary considerably among different inclusion shapes for $\delta=1/10$, 1, and 10, as can be seen from Table II, with discs and spheres yielding the most negative σ_e at $\delta=1/10$, disks and disks at $\delta=1$, and blades and disks at $\delta=10$, in which case one also has $\sigma_e>0$ for both discs and spheres.

The characteristic curves of σ_e vs δ, ϕ, and σ_m, respectively, with other parameters fixed, are shown in Figs. 1–3 for spheres, needles, and disks. As for the first two types of curves, these three inclusion shapes are seen to give the same kind of dependence of σ_e on either δ or ϕ with the exception of disks at $\sigma_m=0.45$ and 0.2, for which a maximum, instead of a minimum, of σ_e is present at a certain value of δ. The dependence of σ_e on σ_m is more varied for different values of δ whether σ_m and σ are equal or not, as shown in Figs. 3 and 4. In particular, from Fig. 4 it is seen that for $\sigma=\sigma_m=1/5$ one has $\sigma_e=1/5$ for spheres and disks for all three values of δ, but for needles only for $\delta=1$ [see also the discussion following Eq. (39)].

For composites of auxetics with both equal and unequal σ_m and σ, different kinds of dependence of σ_e on δ for all five inclusion shapes are compared in Figs. 5 and 6 for $\delta=-0.8$, $\sigma_m=0.25$, and $\phi=0.4$. It is seen from Fig. 5 that in two dimensions σ_e is lower for discs when δ lies approximately between 0.3 and 1.6, but higher otherwise, while in three dimensions a similar interval for spheres is approximately [0.3,0.8], with disks yielding the most negative σ_e at $\delta>1$. For $\sigma=\sigma_m=-0.5$ and $\phi=0.4$, we find from Fig. 6 that for $\delta>2$, discs give lower values of σ_e than blades, while in three dimensions disks give the lowest and needles the highest values.

As revealed in Ref. [3], the effects of interactions among spherical auxetic inclusions on σ_e are simply the slightly widening of auxeticity windows for δ. This is the case for spheres in both two and three dimensions as seen from Fig. 7 with $\sigma=-0.8$, $\sigma_m=0.25$, and $\phi=0.4$.

We have so far discussed the effects on σ_e of only three distinctive types of inclusion shapes: spheres, needles, and disks. It must, however, be pointed out that other nonellipsoidal inclusion shapes such as oblong and convex poly-

gons [41] may also be considered as may fine, cylindrical fibers [33] or even randomly coiled wires [30]. The constraint of perfect bonding between phases in the mean-field approximation may be relaxed by taking into account the bonding imperfections or the interface zones [42]. The effects on σ_e of the matrix being a half space or two joined semi-infinite elastic bodies, a bimaterial, may also be considered [43] as may the extension of the present treatment to the effective electroelastic properties of piezoelectric composites [44] with auxetic inclusions. Even effective micropolar elastic properties may be investigated as micropolar Eshelby tensors for both spherical and cylindrical inclusions have been obtained [45], which recover classical Eshelby tensors as special cases. We thus see that many more challenging problems remain to be solved, especially those associated with accurate theoretical prediction and experimental determination of effective Poisson ratios in composites of auxetics of a higher volume fraction for which both intensive and extensive research on their experimental preparations are under way.

In conclusion, we have given a short but thorough review of the existing mean-field theory of effective elastic properties of disordered composites with ellipsoidal inclusions and indicated how interactions among the inclusions may be taken into account. Extensive analytic and numerical results have been obtained concerning the effects, on effective Poisson ratios of a two-phase composite, of both inclusion shapes and such parameters as inclusion volume or area fraction and Poisson ratio, matrix Poisson ratio, and the ratio of the Young modulus of inclusion to that of the matrix. In particular, the existence of auxeticity windows for composites of auxetic discs, spheres, blades, needles, and disks is demonstrated theoretically and some challenging problems for future work are identified including experimental verification of the predicted existence of the auxeticity windows.

ACKNOWLEDGMENTS

This work was supported in part by the NSF of China and by the FEYUT, SEDC, China. G.Y.W. is thankful for financial support from the Royal Society K. C. Wong Foundation and for the hospitality of Gonville and Caius College, Cambridge. S.F.E. acknowledges financial support from the Emeritus Leverhulme Foundation. The authors are very grateful for the valuable assistance of and fruitful conversations with their colleagues Dr. R. C. Ball, Dr. Mike Cates, Alan Catherall, Dr. T. C. Choy, Dr. Serguei Fridrikh, Hui-Yong Hu, Dr. Steve C. Moratti, Dr. Zemin Ning, Dr. Eugene Terentjev, Dr. Mark Warner, and Professor Xinsheng Zhao.

[1] R. Lakes, Science **235**, 1038 (1987); S. Burns, *ibid.* **238**, 551 (1987).
[2] K. L. Alderson and K. E. Evans, Polymer **33**, 4435 (1992).
[3] G. Y. Wei and S. F. Edwards, Physica A (to be published).
[4] B. U. Felderhof and P. L. Iske, Phys. Rev. A **45**, 611 (1992); B. U. Felderhof, Physica A **207**, 13 (1994).
[5] G. J. Weng, Int. J. Eng. Sci. **22**, 845 (1984); E. H. Kerner, Proc. Phys. Soc. London, Sect. B **69**, 802 (1956); **69**, 808 (1956).
[6] K. Z. Markov, in *Continuum Models of Discrete Systems 4*, edited by O. Brulin and R. K. T. Hsieh (North-Holland, Amsterdam, 1981), p. 441.
[7] T. Mori and K. Tanaka, Acta Metall. **21**, 571 (1973).
[8] Y. Benveniste, Mech. Mater. **6**, 147 (1987).
[9] J. G. Berryman and P. A. Berge, Mech. Mater. **22**, 149 (1996); J. G. Berryman, in *American Geophysical Union Handbook of Physical Constants*, edited by T. J. Ahrens (AGU, New York, 1995), p. 205.
[10] J. D. Eshelby, Proc. R. Soc. London, Ser. A **241**, 376 (1957).
[11] J. A. Reynolds and J. M. Hough, Proc. Phys. Soc. London, Sect. B **70**, 769 (1957).
[12] E. C. Stoner, Philos. Mag. **36**, 803 (1945).
[13] L. Landau, E. M. Lifshitz, and L. P. Pitaevskii, *Electrodynamics of Continuous Media*, 2nd ed. (Pergamon, London, 1984), p. 23.
[14] J. A. Osborn, Phys. Rev. **67**, 351 (1945).
[15] T. C. Choy and A. M. Stoneham, J. Phys.: Condens. Matter **2**, 939 (1990).
[16] T. W. Noh, P. H. Song, and A. J. Sievers, Phys. Rev. B **44**, 5459 (1991).
[17] H. Fricke, Phys. Rev. **24**, 575 (1924).
[18] D. A. G. Bruggeman, Ann. Phys. (Leipzig) **24**, 636 (1935).
[19] R. Hill, J. Mech. Phys. Solids **11**, 357 (1963).
[20] T. Wu, Int. J. Solids Struct. **2**, 1 (1966); L. J. Walpole, J. Mech. Phys. Solids **17**, 235 (1969); S. Boucher, J. Compos. Mater. **8**, 82 (1974).
[21] J. G. Berryman, J. Acoust. Soc. Am. **68**, 1809 (1980); **68**, 1820 (1980); G. T. Kuster and M. N. Toksz, Geophysics **39**, 587 (1974).
[22] S. Torquato, J. Mech. Phys. Solids **45**, 1421 (1997); Phys. Rev. Lett. **79**, 681 (1997).
[23] Z. Hashin and S. Shtrikman, J. Mech. Phys. Solids **11**, 127 (1963); L. J. Walpole, Q. J. Mech. Appl. Math. **25**, 153 (1972); M. Reiner, in *Encyclopedia of Physics VI* (Springer, Berlin, 1958), p. 528.
[24] J. G. Kirkwood, J. Chem. Phys. **4**, 592 (1936).
[25] W. F. Brown, Jr., J. Chem. Phys. **23**, 1514 (1955).
[26] B. U. Felderhof, G. W. Ford, and E. G. D. Cohen, J. Stat. Phys. **28**, 135 (1982); B. Cichocki and B. U. Felderhof, *ibid.* **53**, 499 (1988).
[27] S. Torquato, J. Appl. Phys. **58**, 3790 (1985); A. K. Sen and S. Torquato, Phys. Rev. B **39**, 4504 (1989).
[28] R. W. Zimmerman, Mech. Res. Commun. **19**, 563 (1992).
[29] M. N. Miller, J. Math. Phys. **10**, 2005 (1969).
[30] S. F. Edwards and A. G. Miller, J. Phys. D **9**, 555 (1976).
[31] J. R. Willis, Adv. Appl. Mech. **21**, 1 (1981); L. J. Walpole, *ibid.*, **21**, 169 (1981).
[32] R. B. Jones and R. Schmitz, Physica A **122**, 105 (1983); **122**, 114 (1983); **125**, 381 (1984); **126**, 1 (1984).
[33] M. E. Cates and S. F. Edwards, Proc. R. Soc. London, Ser. A **395**, 89 (1984).
[34] M. F. Thorpe and P. N. Sen, J. Acoust. Soc. Am. **77**, 1674 (1985).

[35] F. Lado and S. Torquato, J. Chem. Phys. **93**, 5912 (1990).
[36] J. W. Ju and T. M. Chen, Acta Mech. **103**, 103 (1994); **103**, 123 (1994); E. J. Garboczi and J. F. Douglas, Phys. Rev. E **53**, 6169 (1996).
[37] S. Torquato, Appl. Mech. Rev. **44**, 37 (1991); F. Lado, J. Chem. Phys. **49**, 3092 (1968); L. Verlet and J.-J. Weis, Phys. Rev. A **5**, 939 (1972).
[38] B. U. Felderhof, J. Phys. C **15**, 3943 (1982); **15**, 3953 (1982); B.U. Felderhof, G. W. Ford, and E. G. D. Cohen, J. Stat. Phys. **28**, 135 (1982); **28**, 649 (1982).
[39] J. D. Beasley and S. Torquato, J. Appl. Phys. **60**, 3576 (1986); S. Torquato and F. Lado, Proc. R. Soc. London, Ser. A **417**, 59 (1988); J. Appl. Mech. **59**, 1 (1992).
[40] W. L. Bragg and A. B. Pippard, Acta Crystallogr. **6**, 865 (1953); J. L. Oncley, Ann. (N.Y.) Acad. Sci. **41**, 121 (1941).
[41] H. Nozaki and M. Taya, J. Appl. Mech. **64**, 495 (1997); F. C. Chen and K. Young, J. Math. Phys. **18**, 1412 (1977).
[42] Z. Zhong and S. A. Meguid, J. Elast. **46**, 91 (1997); A. Al-Ostaz and I. Jasiuk, Acta Mater. **45**, 4131 (1996); M. P. Lutz and R. W. Zimmerman, J. Appl. Mech. **63**, 855 (1996); T. Chen, J. Mech. Phys. Solids **45**, 385 (1997); A. S. Sangani and G. Mo, *ibid.* **45**, 2001 (1997).
[43] H. Y. Yu and S. C. Sanday, Proc. R. Soc. London, Ser. A **439**, 659 (1992); I. Jasiuk, P. Y. Sheng, and E. Tsuchida, J. Appl. Mech. **64**, 471 (1997).
[44] W.-S. Kuo and J. H. Huang, Int. J. Solids Struct. **34**, 2445 (1997); M. L. Dunn and H. A. Wienecke, *ibid.* **34**, 3571 (1997); L. V. Gibiansky and S. Torquato, J. Mech. Phys. Solids **45**, 689 (1997); J. G. Berryman, Phys. Rev. Lett. **79**, 1142 (1997).
[45] Z.-H. Cheng and L.-H. He, Int. J. Eng. Sci. **33**, 389 (1995); **35**, 659 (1997); Acta Mech. **116**, 97 (1996).